A Study of the Long Atmospheric Waves on the Basis of Zonal Harmonic Analysis

By E. ELIASEN, University of Copenhagen

(Manuscript received June 17, 1957)

Abstract

Characteristic features of the long atmospheric waves at middle latitudes are discussed on the basis of zonal harmonic analyses of hemispherical weather charts. In the first section mean values of the amplitudes of the waves with wavenumbers from 1 to 10 are presented for the 500-mb and the 1000-mb levels. Spectral distributions of the kinetic energy for the eastward and the northward components of the geostrophic wind at the 500-mb level are computed. In section 2 the semi-permanence of the waves with wavenumbers from 1 to 4 is illustrated. The meridional variation of the waves is investigated in relation to the question about the meridional transport of momentum. On the basis of the vertical variations of the waves of the January and July normal charts the causes of the semi-permanent waves are discussed. The travelling waves with wavenumbers 5, 6, and 7 are treated in section 3. Mean speeds of the waves are considered in relation to the mean velocity of the zonal flow. The vertical structure of the waves is investigated by means of the heights of the 1000-mb and 500-mb levels and the temperature field at the 500-mb level. Finally the speed and vertical structure of the waves are determined theoretically from the solutions of the linear equations in a two-level approximation.

Introduction

The atmospheric motion as it presents itself on hemispherical weather charts can be considered immediately as a zonal flow upon which are superimposed more or less marked disturbances. The disturbances, however, represent again a superposition of components with horizontal scales in a very wide range. The most simple, quantitative analysis of the components with the largest scales (wavelengths larger than about 3,000 km) seems to be performed by a decomposition into waves with different wavelengths in the zonal direction.

In the following the results of a series of such analyses of actual weather charts are presented in order to outline certain characteristic features related to the different wavelengths, especially the distribution of kinetic energy, the types of motion and the meridional and vertical structure of the waves in the lower and middle troposphere. The analyses have been carried out once a day for the period 21 October to 30 November 1950 on the basis of the 1,000-mb and 500-mb charts from "Daily Series Synoptic Weather Maps" published by U.S. Weather Bureau. Furthermore the investigation includes certain normal charts from "Normal Weather Charts for the Northern Hemisphere", U.S. Weather Bureau, 1952.

1. The spectral distribution of kinetic energy

By a zonal harmonic analysis the height z of a pressure surface as function of the longitude ϑ and the latitude φ can be written

$$z(\varphi, \vartheta) = \bar{z}(\varphi) + \sum_m \{a_m(\varphi) \cos m\vartheta + b_m(\varphi) \sin m\vartheta\},$$
$$m = 1, 2, - - \qquad (1)$$

with

$$\bar{z}(\varphi) = \frac{1}{2\pi} \int_0^{2\pi} z(\varphi, \vartheta)\, d\vartheta$$

$$a_m(\varphi) = \frac{1}{\pi} \int_0^{2\pi} z(\varphi, \vartheta) \cos m\vartheta\, d\vartheta,$$

$$b_m(\varphi) = \frac{1}{\pi} \int_0^{2\pi} z(\varphi, \vartheta) \sin m\vartheta\, d\vartheta$$

The values of a_m and b_m have been computed by approximating the integrals round the latitude circles by the corresponding sums of the values for each five degrees of longitude.

Table 1. Mean values of A_m in m.

m	500 mb			1,000 mb
	40° N	50° N	60° N	50° N
1	49	86	111	72
2	46	76	109	54
3	43	96	92	53
4	57	58	58	36
5	58	68	54	35
6	38	45	30	31
7	37	39	29	23
8	21	25	14	17
9	19	22	14	15
10	10	16	13	13

Table 1 shows the mean values over the period 21 October to 30 November of the amplitudes $A_m = \sqrt{a_m^2 + b_m^2}$ for the wavenumbers from 1 to 10. For the 500-mb level the values are given at the latitudes 40, 50 and 60° N, and for the 1.000-mb level at 50° N. Generally the amplitudes are small to the south of 30° N and for $m > 3$ also to the north of 70° N. For $m \leq 3$ the amplitudes have their maximum values to the north of 50° N, while for $m \geq 5$ they have their maxima between 45 and 50° N. The ratio between the amplitude at the 1,000-mb level and the amplitude at the 500-mb level has at 50° N the largest values for $m = 1$ (0.84) and $m = 10$ (0.81) and the smallest value for $m = 5$ (0.52).

From the height of the pressure surface we get the following components of the geostrophic wind in the eastward and in the northward direction.

$$u = -\frac{g}{2\Omega \sin\varphi} \frac{\partial z}{r\partial\varphi}, \quad v = \frac{g}{2\Omega \sin\varphi} \frac{\partial z}{r \cos\varphi \partial\vartheta} \qquad (2)$$

where g is the acceleration of gravity, r the radius and Ω the angular velocity of the earth. The decomposition of u and v corresponding to (1) becomes

$$\left.\begin{aligned} u(\varphi, \vartheta) &= \bar{u}(\varphi) + \\ &+ \sum_m \{a_m^{(u)}(\varphi) \cos m\vartheta + b_m^{(u)}(\varphi) \sin m\vartheta\} \\ v(\varphi, \vartheta) &= \\ &= \sum_m \{a_m^{(v)}(\varphi) \cos m\vartheta + b_m^{(v)}(\varphi) \sin m\vartheta\} \end{aligned}\right\} \qquad (3)$$

where the mean zonal velocity $\bar{u}(\varphi)$ is given by

$$\bar{u}(\varphi) = \frac{1}{2\pi} \int_0^{2\pi} u(\varphi, \vartheta)\, d\vartheta = -\frac{g}{2\Omega r \sin\varphi} \frac{\partial \bar{z}}{\partial\varphi} \qquad (4)$$

and where

$$\left.\begin{aligned} a_m^{(u)} &= -\frac{g}{2\Omega r \sin\varphi} \frac{\partial a_m}{\partial\varphi}, \\ b_m^{(u)} &= -\frac{g}{2\Omega r \sin\vartheta} \frac{\partial b_m}{\partial\varphi} \\ a_m^{(v)} &= +\frac{g}{2\Omega r \sin\varphi \cos\varphi} m b_m, \\ b_m^{(v)} &= -\frac{g}{2\Omega r \sin\varphi \cos\varphi} m a_m \end{aligned}\right\} \qquad (5)$$

The relative importance of the different wavenumbers can perhaps best be expressed by the spectral distribution of the kinetic energy or of the density of $\frac{1}{2}(u^2 + v^2)$ (cf. the discussion of the energy spectrum of the meridional motion for the period December 1949—February 1950 by White and Cooley, 1956). From (3) we get

$$\frac{1}{2\pi} \int_0^{2\pi} \frac{1}{2}(u^2 + v^2)\, d\vartheta = e_0^{(u)} + \sum_m \{e_m^{(u)} + e_m^{(v)}\} \qquad (6)$$

with

$$\left.\begin{aligned} e_0^{(u)} &= \frac{1}{2} \bar{u}^2 \\ e_m^{(u)} &= \frac{1}{4}\{a_m^{(u)2} + b_m^{(u)2}\}, \quad e_m^{(v)} = \frac{1}{4}\{a_m^{(v)2} + b_m^{(v)2}\} \end{aligned}\right\} \qquad (7)$$

These quantities have been computed at the latitudes 37½, 47½ and 57½° N using

$$\left.\begin{aligned} a_m(\varphi) &= \frac{1}{2}\left\{a_m\left(\varphi+\frac{\pi}{72}\right)+a_m\left(\varphi-\frac{\pi}{72}\right)\right\} \\ \frac{\partial a_m}{\partial \varphi} &= \frac{36}{\pi}\left\{a_m\left(\varphi+\frac{\pi}{72}\right)-a_m\left(\varphi-\frac{\pi}{72}\right)\right\} \end{aligned}\right\} \quad (8)$$

and the corresponding expressions for $b_m(\varphi)$ and $\frac{\partial b_m}{\partial \varphi}$. The mean values for the 14 days 21 October, 24 October, — — —, 29 November 1950 are shown in Fig. 1, where the lower part of the columns represents the values of $e_m^{(u)}$ and the upper part the values of $e_m^{(v)}$. It is seen that $e_m = e_m^{(u)} + e_m^{(v)}$ has a maximum for $m = 5$, which at 47½° N corresponds nearly to the wavelength 5.400 km. For $m > 5$ e_m decreases rather rapidly with increasing m, whereas for $m < 5$ the variation is different at the three latitudes. Table 2 gives a comparison between the kinetic energy contained in the zonal flow, the waves with m from 1 to 4 and the waves with m from 5 to 10. For each of the two groups of waves the energy is of the same order of magnitude. To the south of about 50° N the kinetic energy of the zonal flow is larger than the total kinetic energy of the waves, whereas to the north it becomes essentially smaller.

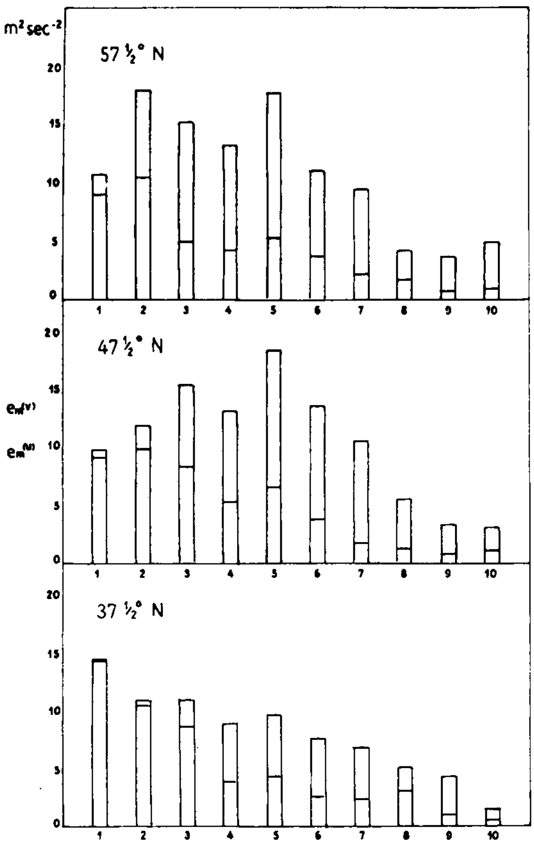

Fig. 1. Spectral distribution of kinetic energy at the 500-mb level during the period 21 October—30 November 1950. The lower part of the columns, $e_m^{(u)}$, represents the contributions from the eastward and the upper part of the columns, $e_m^{(v)}$, the contributions from the northward component of the geostrophic wind.

Table 2. Mean values of e_m in m² sec⁻² (500-mb level).

	37½° N	47½° N	57½° N
e_0	112	172	37
$\sum_{m=1}^{4} e_m$	44	50	57
$\sum_{m=5}^{10} e_m$	35	56	51

From Fig. 1 it is further seen that for $m = 1$ and 2 essentially more energy is contained in the u-component than it the v-component of the velocity, whereas for $m \geqq 4$ most of the energy is contained in the v-component. This indicates that the scale in the south-north direction, expressed by a "characteristic wavelength", will be smaller than the wavelength in the west-east direction for $m = 1$ and 2, whereas it will be larger for $m \geqq 4$.

2. The long semi-permanent waves

In order to examine the day-to-day variations of the different waves we write

$$\begin{aligned} a_m(\varphi, t)\cos m\vartheta + b_m(\varphi, t)\sin m\vartheta &= \\ = A_m(\varphi, t)\cos m\{\vartheta - \delta_m(\varphi, t)\} & \quad (9) \end{aligned}$$

where the phase angle $\delta_m(\varphi, t)$ states the position of a ridge. The motion at the 500-mb level of the longest waves, $m = 1, 2, 3$ and 4, is illustrated in Fig. 2, showing δ_m as function of time at the latitude 50° N. It is seen that each of the waves fluctuates about a certain mean position, and only in some few cases the deviation from the mean position becomes larger than a quarter of the wavelength. Oc-

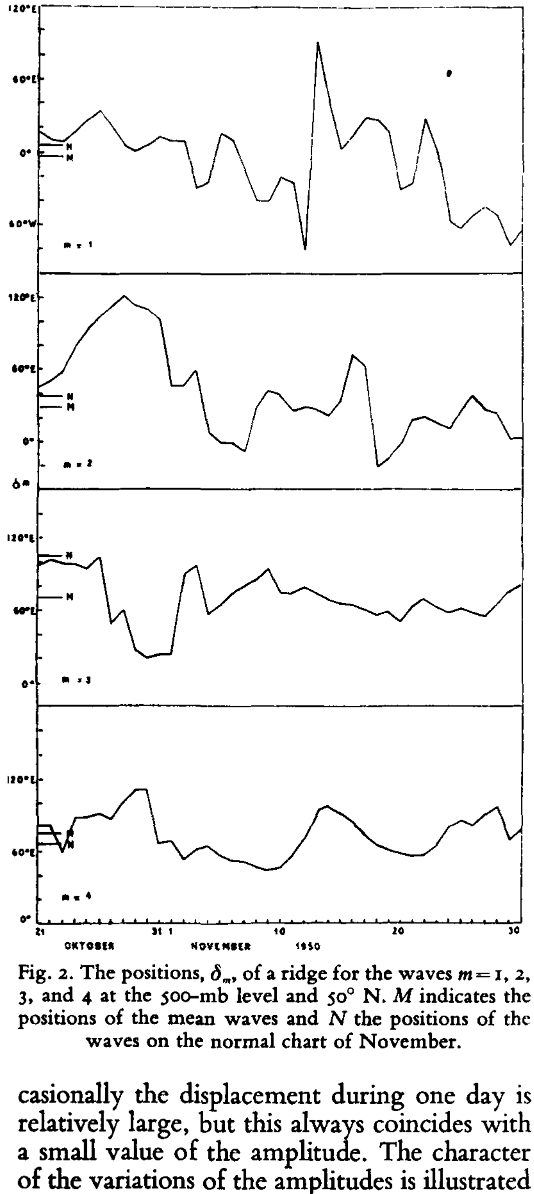

Fig. 2. The positions, δ_m, of a ridge for the waves $m = 1$, 2, 3, and 4 at the 500-mb level and 50° N. M indicates the positions of the mean waves and N the positions of the waves on the normal chart of November.

casionally the displacement during one day is relatively large, but this always coincides with a small value of the amplitude. The character of the variations of the amplitudes is illustrated in Fig. 3, which shows the values of the amplitude for $m = 3$ as function of time. The standard deviations of the amplitudes are for $m = 1$: 31, for $m = 2$: 41, for $m = 3$: 37 and for $m = 4$: 25 meters.

As a consequence of the semi-permanence these long waves are maintained on the monthly mean charts. They are also present on the normal charts for the individual months, which indicates that the mean positions of the waves are nearly the same from year to year.

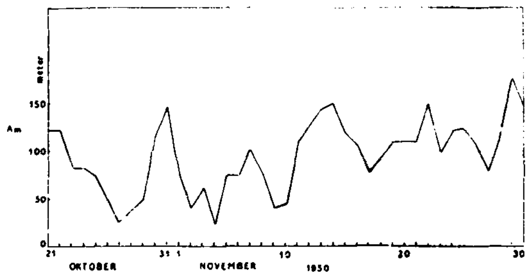

Fig. 3. The values of the amplitude A_m for $m = 3$ at the 500-mb level and 50° N.

For the mean over the period 21 October—30 November 1950 the amplitudes and phase angles of the waves with m from 1 to 5 are shown in Table 3 for the 500-mb and 1,000-mb levels at the latitude 50° N. For $m = 1$ the amplitude of the mean wave is about 3/4 times the mean of the amplitudes (Table 1), else the amplitudes of the mean waves are about the half of the mean values of the amplitudes. This is also seen to be the case for $m = 5$ (cf. the next section), whereas the waves with $m \geq 6$ almost vanish in the mean. For comparison Table 4 contains the result of the corresponding harmonic analysis of the normal charts for the month of November. In Fig. 2 the positions of the mean waves (Table 3) are marked by M and the positions of the normal waves (Table 4) by N.

Table 3. The mean waves at 50° N. A_m in m and δ_m in degrees of longitude.

m	500 mb		1,000 mb	
	A_m	δ_m	A_m	δ_m
1	72	356	63	84
2	41	29	40	92
3	54	70	22	73
4	24	76	14	85
5	37	32	18	0

Table 4. The waves of the normal charts of November at 50°N. A_m in m and δ_m in degrees of longitude.

m	500 mb		1,000 mb	
	A_m	δ_m	A_m	δ_m
1	98	6	60	62
2	53	38	59	84
3	41	105	12	120
4	20	67	4	74
5	15	30	8	33

Table 5. Harmonic analysis of normal charts. A_m in m and δ_m in degrees of longitude.

Latitude	m	January				July			
		500 mb		1,000 mb		500 mb		1,000 mb	
		A_m	δ_m	A_m	δ_m	A_m	δ_m	A_m	δ_m
30° N	1	59	292	16	351	41	312	79	256
	2	10	145	16	110	16	175	53	165
	3	28	83	17	102	4	17	21	77
40° N	1	84	326	39	46	38	332	66	262
	2	34	42	48	89	12	77	48	179
	3	64	98	32	108	12	79	22	83
50° N	1	84	6	76	66	32	22	38	271
	2	79	43	83	85	43	73	32	14
	3	80	106	33	2	22	111	12	93
60° N	1	62	40	71	114	35	73	17	259
	2	100	33	64	79	42	58	19	30
	3	63	108	43	12	24	114	6	104
70° N	1	50	84	87	163	39	116	3	274
	2	98	21	19	71	40	40	12	23
	3	40	108	18	3	14	101	2	110

The motion of the waves has also been investigated at the latitudes 40 and 60° N, and it parallels rather closely the motion at 50° N, with a certain tilt of the trough- and ridge-lines. The meridional variation of the waves $m = 1$, 2 and 3 on the normal charts of January and July can be seen from Table 5, giving the values of A_m and δ_m at the latitudes 30, 40, 50, 60 and 70° N for the 500-mb and 1,000-mb levels. The tilt of the trough- and ridge-lines is decisive for the meridional transport of momentum in the way that the waves with SW—NE orientation of the axes give a northward transport whereas the waves with SE—NW orientation give a southward transport. With the decomposition (3) we get

$$\left.\begin{aligned} \tau &= \frac{1}{2\pi}\int_0^{2\pi} u\,v\,d\vartheta = \sum_m \tau_m \\ \tau_m &= \frac{1}{2}\{a_m^{(u)}\,a_m^{(v)} + b_m^{(u)} b_m^{(v)}\} \end{aligned}\right\} \qquad (10)$$

Using (5) and (8) τ_m has been computed from the 500-mb and 1,000-mb normal charts for January and July. The values for $m = 1$, 2 and 3 at the latitudes 27½, 37½, 47½ and 57½° N are listed in Table 6. The values for $m \geqq 4$ are quite insignificant.

A comparison with the total mean transport τ computed for instance for January 1949 by MINTZ (1951) indicates that the transport connected with the long semi-permanent waves is by no means negligible (cf. STARR and WHITE, 1952). For January 1949 the mean of τ has at the 500-mb level the maximum value

Table 6. τ_m for the normal charts in $m^2\,sec^{-2}$.

Latitude	m	January		July	
		500 mb	1000 mb	500 mb	1000 mb
27½° N	1	0.9	0.3	—0.1	0.3
	2	0.2	—0.6	0.1	2.0
	3	4.1	0.6	—0.2	0.7
37½° N	1	5.0	0.6	0.6	0.5
	2	0.5	—1.7	—0.1	2.9
	3	5.5	0.8	0.1	0.5
47½° N	1	4.2	1.2	1.1	0.3
	2	—0.5	—0.6	0.0	1.1
	3	5.2	2.4	0.2	0.4
57½° N	1	2.3	4.4	0.8	—0.1
	2	—4.8	—2.2	—1.8	0.5
	3	1.5	1.2	—0.3	0.1
67½° N	1	1.7	4.3	0.6	0.0
	2	—9.6	—0.3	—2.4	—0.3
	3	—0.5	—1.7	—0.2	0.0

36 $m^2 sec^{-2}$ at about 40° N, and the corresponding total value for the long waves on the normal chart becomes 12 $m^2 sec^{-2}$.

The existence of the long semi-permanent waves is presumably explained as the combined effect of the large-scale distribution of heat sources and the large mountain barriers (the Rocky Mountains and the mountains in the interior of Asia). Largely the continents act as cold sources and the oceans as warm sources in winter and inversely in summer. This should indicate a phase shift for the corresponding waves during the year. The normal positions in the lower and middle troposphere of the waves $m = 1$, 2 and 3 in the months of January and July are therefore placed together in Fig. 4 for the latitude 50° N on

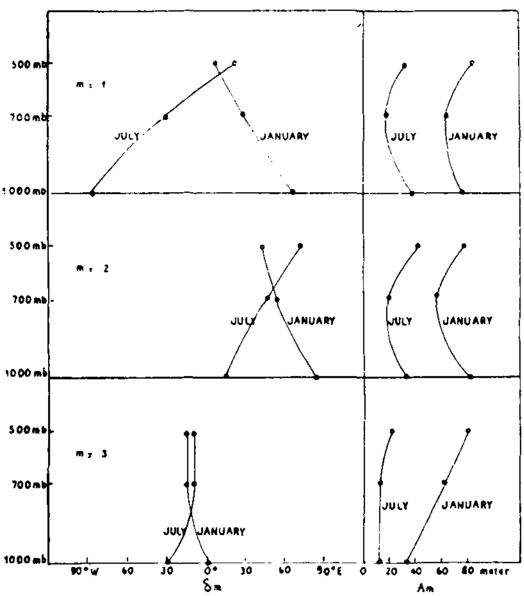

Fig. 4. Harmonic analysis of the normal charts of January and July at 50° N. The positions, δ_m, of a ridge and the values, A , of the amplitude for the waves $m=1$, 2, and 3 at the 1,000-mb, 700-mb and 500-mb levels.

the basis of the harmonic analysis of the normal charts for the 500-mb, 700-mb and 1,000-mb levels. The figure also shows the corresponding values of the amplitudes. In the lowest layer of the troposphere the phase differences between January and July are considerably, namely for $m = 1: 0.43$, for $m = 2: 0.39$ and for $m = 3: 0.24$ times the wavelength. This is at least qualitatively in agreement with the phase shift of the heat sources. However, in the layer from 700 mb to 500 mb the phase differences become much smaller, which constitutes an essential argument (CHARNEY and ELIASSEN, 1949) for ascribing the large mountain barriers an essential role.

The effect of the heat sources has been studied by SMAGORINSKY (1953) on the basis of the linear equations, and it seems likely that the amplitudes of the waves caused by the heat sources will be rather constant or even decrease with height. The perturbations caused by the mountain barriers have been investigated for the equivalent-barotropic level by CHARNEY and ELIASSEN (1949) and BOLIN (1950) and a considerable agreement with the real perturbations at the 500-mb level has been demonstrated. Extending the computations to a baroclinic atmosphere, utilizing the confluent hypergeometric functions tabulated by CHARNEY (1947), it turns out that the amplitudes of the orographically induced waves increase essentially with height, the amplitudes at the 500-mb level being between 2 and 3 times the amplitudes at the 1,000-mb level. So it seems that the large-scale distribution of heat sources plays an important role in the formation of the long waves in the lowest part of the troposphere, whereas the effect of the large mountain barriers becomes predominant in the middle and upper troposphere.

3. The travelling waves

The day-to-day variations of the wave with wavenumber 5 at the 500-mb level and at 50° N are shown in Fig. 5. In the periods 21—27 October and 5—20 November the wave moves towards the east with a speed of about 9 degrees of longitude per day. On the other hand, from 27 October to 5 November and from 20 to 30 November the wave is quasi-stationary in a position coinciding very nearly with the position of the wave on the normal chart of November, marked N (Table 4). The values of the amplitude are shown in the upper part of the figure, but (as for the other m) there seems to be no, at least no simple, relation between the motion of the wave and its amplitude.

The waves with wavenumber larger than 5 seem to move consistently towards the east.

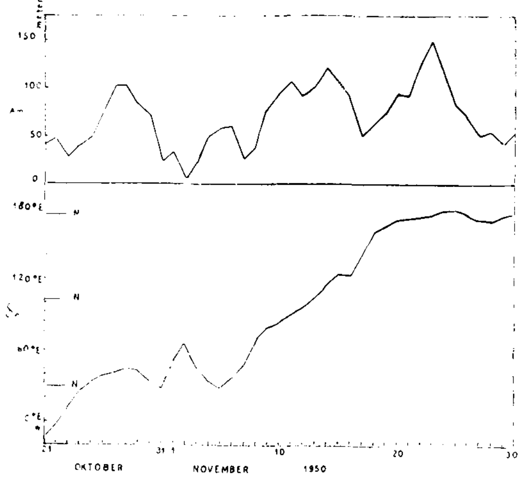

Fig. 5. The positions, δ_m, of a ridge and the values, A_m, of the amplitude for the wave $m = 5$ at the 500-mb level and 50° N. N indicates the position of the wave on the normal chart of November.

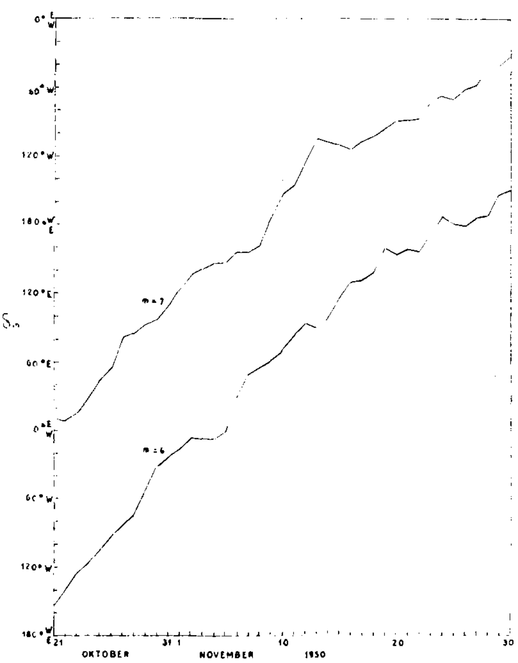

Fig. 6. The positions, δ_m, of a ridge for the waves $m = 6$ and 7 at the 500-mb level and 50° N.

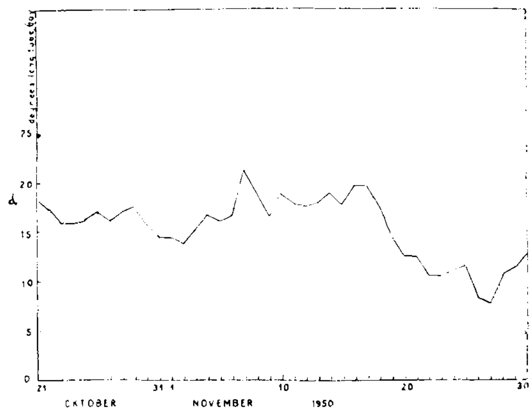

Fig. 7. The mean angular velocity, α, of the zonal flow in the belt from 40 to 60° N at the 500-mb level.

The motion for $m = 6$ and 7 is shown in Fig. 6, still for the 500-mb level and at 50° N. It is seen that there is no essential difference between the motion of the two waves. During the period from 23 October to 15 November they move with the same mean speed of nearly 10 degrees of longitude per day, whereas from 18 to 30 November the common mean speed is only about 6 degrees of longitude per day. This decrease in the speed of the waves seems to be related to a corresponding decrease of the angular velocity α of the zonal flow, which can be seen from Fig. 7. The values of α are computed as the geostrophic values at 50° N, using the mean gradients of $\bar{z}(\varphi)$ between 40 and 60° N. The mean value of α for the period 23 October to 15 November is 16.7 and for the period 18 to 30 November 11.7 degrees of longitude per day.

The standard deviations of the amplitudes (500 mb, 50° N) become for $m = 5$: 33, for $m = 6$: 21 and for $m = 7$: 20 meters, i.e. in all three cases nearly 0.5 times the mean value of the amplitude.

The motion of the wave $m = 8$ shows a very similar picture. However, with decreasing wavelength the displacements of the waves during one day often become of the same magnitude as half of the wavelength, leading to ambiguities in the fixing of the motion.

The motion of the waves $m = 5$, 6 and 7 at the latitudes 40 and 60° N follows largely the motion at 50° N. In nearly 50 per cent of the cases the phase difference between 40 and 50° N as well as between 50 and 60° N is smaller than 5 degrees of longitude and in about 75 per cent of the cases it is smaller than 10 degrees. For both $m = 5$ and 6 there is from 40 to 60° N a SW—NE tilt of the trough- and ridge-lines in nearly 60 per cent of the cases, but for $m = 7$ in only 40 per cent. However, for all three values of m the mean values of the phase differences between 40, 50 and 60° N become quite insignificant.

The relation between the mean of the amplitudes for the wave at the 500-mb and the 1,000-mb levels has been shown for 50° N in Table 1. For $m = 5$, 6 and 7 the correlation coefficients of the amplitudes at the two levels are about 0.50. The distribution during the 41 days of the phase differences, $\triangle_1$, from the waves at the 500-mb level to the waves at the 1,000-mb level is shown for 50° N in Table 7. It is seen that in the mean the waves

Table 7. Distribution of $\triangle_1$. Number of cases.

	$m = 5$	$m = 6$	$m = 7$
$-27 \leqq \triangle_1 \leqq -23$	1	0	0
$-22 \leqq \triangle_1 \leqq -18$	0	1	1
$-17 \leqq \triangle_1 \leqq -13$	1	0	1
$-12 \leqq \triangle_1 \leqq -8$	3	2	0
$-7 \leqq \triangle_1 \leqq -3$	2	2	2
$-2 \leqq \triangle_1 \leqq +2$	3	7	9
$3 \leqq \triangle_1 \leqq 7$	11	11	17
$8 \leqq \triangle_1 \leqq 12$	13	10	9
$13 \leqq \triangle_1 \leqq 17$	4	6	2
$18 \leqq \triangle_1 \leqq 22$	1	1	0
$23 \leqq \triangle_1 \leqq 27$	2	1	0

are displaced somewhat to the west at the 500-mb level in relation to the 1,000-mb level. The mean of the phase differences decreases with increasing wavenumber, being approximately 1/10 of the wavelength. For the waves in the thickness field from 1,000 to 500 mb the mean values of the amplitudes become for $m = 5$: 0.84, for $m = 6$: 0.82 and for $m = 7$: 0.74 times the corresponding mean amplitudes of the waves at the 500-mb level. In about 80 per cent of the cases the waves $m = 5$, 6 and 7 in the thickness field are displaced towards the west in relation to the waves at the 500-mb level, the mean displacements amounting to about 5 degrees of longitude. The distribution of the displacements (towards the west), $\triangle_2$, is shown in Table 8.

The vertical structure of the waves can be further investigated by harmonic analysis of the temperature field T at the 500-mb level. The positions of the waves $m = 5$, 6 and 7 in this temperature field correspond in the mean very nearly with the positions in the

Table 8. Distribution of $\triangle_2$. Number of cases.

	$m = 5$	$m = 6$	$m = 7$
$-27 \leqq \triangle_2 \leqq -23$	0	0	0
$-22 \leqq \triangle_2 \leqq -18$	0	1	0
$-17 \leqq \triangle_2 \leqq -13$	0	1	0
$-12 \leqq \triangle_2 \leqq -8$	0	2	1
$-7 \leqq \triangle_2 \leqq -3$	4	2	2
$-2 \leqq \triangle_2 \leqq +2$	6	7	9
$3 \leqq \triangle_2 \leqq 7$	22	17	20
$8 \leqq \triangle_2 \leqq 12$	6	6	5
$13 \leqq \triangle_2 \leqq 17$	2	2	3
$18 \leqq \triangle_2 \leqq 22$	0	1	1
$23 \leqq \triangle_2 \leqq 27$	1	2	0

thickness field from 1,000 to 500 mb, the westward displacements relatively to the positions at the 500-mb level being slightly smaller. Writing

$$T(\varphi, \vartheta) = \overline{T}(\varphi) + \sum_m \{a_m^{(T)}(\varphi) \cos m\vartheta + b_m^{(T)} \sin m\vartheta\} \qquad (11)$$

we get from the hydrostatic equation

$$\frac{\partial a_m}{\partial p} = -\frac{R}{gp} a_m^{(T)}, \quad \frac{\partial b_m}{\partial p} = -\frac{R}{gp} b_m^{(T)} \qquad (12)$$

where R is the gas constant of air. Introducing the thickness field

$$h = -\frac{\partial z}{\partial p} \triangle p = \overline{h} + \sum \{a_m^{(h)} \cos m\vartheta + b_m^{(h)} \sin m\vartheta\} \qquad (13)$$

with $\triangle p = 100$ mb, we get

$$a_m^{(h)} = \frac{R \triangle p}{gp} a_m^{(T)}, \quad b_m^{(h)} = \frac{R \triangle p}{gp} b_m^{(T)} \qquad (14)$$

The mean value of the amplitudes in this thickness field becomes at 50° N for $m = 5$: 0.24, for $m = 6$: 0.29 and for $m = 7$: 0.26 times the corresponding mean amplitudes of the waves at the 500-mb level.

Theoretical investigations (Charney, 1947; Eady, 1949 and Fjørtoft, 1950) based upon solutions of the linear equations for wave motions in a baroclinic zonal current have demonstrated the possible development of long waves transforming potential and internal energy into kinetic energy. Certainly the interactions between the different waves play an important role in the actual atmospheric developments, but owing to the relatively large velocity of the zonal flow and the steadiness of its effect it seems reasonable to suppose that the mean conditions of the waves are decisively influenced by the interaction with the zonal flow. So it may be of some interest to compare the solutions of the linear equations with the mean conditions of the actual waves.

In order to avoid mathematical troubles approximations concerning the vertical variations may be introduced, cf. for instance ELIASSEN (1952) and THOMPSON (1953). Following the method of finite differences by CHARNEY and PHILLIPS (1953) we have for the quasi-geostrophic motion at the two levels p_1 and p_2

$$\left.\begin{aligned}&\left(\frac{\partial}{\partial t}+\mathbf{v}_1\cdot\nabla\right)\left(\xi_1+2\Omega\sin\varphi\right)-\\&-\varkappa\frac{g}{2\Omega\sin\varphi}\left(\frac{\partial}{\partial t}+\mathbf{v}_1\cdot\nabla\right)\left(z_1-z_2\right)=0\\&\left(\frac{\partial}{\partial t}+\mathbf{v}_2\cdot\Delta\right)\left(\xi_2+2\Omega\sin\varphi\right)+\\&+\varkappa\frac{g}{2\Omega\sin\varphi}\left(\frac{\partial}{\partial t}+\mathbf{v}_2\cdot\nabla\right)\left(z_1-z_2\right)=0\end{aligned}\right\}\quad(15)$$

with the vector $\mathbf{v}$ given by (2),

$$\xi=\frac{g}{2\Omega\sin\varphi}\nabla^2 z$$

and

$$\varkappa=-\frac{4\Omega^2\sin^2\varphi}{(p_2-p_1)^2}\left\{\frac{1}{\varrho}\frac{\partial\log\Theta}{\partial p}\right\}^{-1}_{p=\frac{p_1+p_2}{2}}$$

where ϱ is the density and Θ the potential temperature. ∇ denote the spherical del-operator. Approximating the stabilizing influence of the stratosphere on the tropospheric motion by a rigid top placed a little higher than the tropopause, the levels p_1 and p_2 become nearly the 400-mb and the 800-mb levels (cf. BOLIN, 1953). Corresponding to normal conditions $\varkappa$ then has a value equal to or somewhat smaller than $3\cdot10^{-12}\,m^{-2}$ and is treated as a constant.

We now consider a zonal flow with the angular velocity α upon which is superimposed the wave motion

$$z'(\varphi,\vartheta,p,t)=k(p)P_n^m(\sin\varphi)\,e^{im(\vartheta-\gamma t)}\quad(16)$$

where $P_n^m(\sin\varphi)$ denotes the associated Legendre functions of order m and degree n. Neglecting the meridional variation of α we get from (15) the following linear equations

$$\left.\begin{aligned}\{\alpha_1-\gamma-\gamma^\star+q(\alpha_2-\gamma)\}z_1'-q(\alpha_1-\gamma)z_2'=0\\\{\alpha_2-\gamma-\gamma^\star+q(\alpha_1-\gamma)\}z_2'-q(\alpha_2-\gamma)z_2'=0\end{aligned}\right\}\quad(17)$$

where

$$\gamma^\star=\frac{2\Omega}{n(n+1)}\approx\frac{2\Omega+\alpha}{n(n+1)}$$

and

$$q=\frac{\varkappa r^2}{n(n+1)}$$

These equations determine the following values of γ

$$\gamma=\frac{\alpha_1+\alpha_2}{2}-\frac{1+q}{1+2q}\gamma^\star\pm$$
$$\pm\frac{1}{1+2q}\sqrt{q^2\gamma^{\star2}+\frac{1-4q^2}{4}(\alpha_1-\alpha_2)^2}\quad(18)$$

This expression demonstrates the existence of the amplified waves with horizontal scales fixed by the conditions

$$\left.\begin{aligned}n^2(n+1)^2>2\varkappa^2r^4\left(1-\sqrt{1-\frac{4\Omega^2}{\varkappa^2r^4(\alpha_1-\alpha_2)^2}}\right)\\n^2(n+1)^2<2\varkappa^2r^4\left(1+\sqrt{1-\frac{4\Omega^2}{\varkappa^2r^4(\alpha_1-\alpha^2)^2}}\right)\end{aligned}\right\}\quad(19)$$

which with the values of $\alpha_1-\alpha_2$ and $\varkappa$ used in the following become $7<n<15$. As we may assume that it is the energy transforming processes underlying the amplification which, in the mean, maintain the waves against frictional dissipation it seems reasonable to compare just the amplified waves with the actual waves in the atmosphere.

The accuracy of the above two-level approximation was tested by a comparison with the solutions obtained by including more levels in the description of the vertical variation. Introducing four levels we get instead of (17) four equations and consequently four solutions. For the relatively large horizontal scales here considered two of these solutions agree quite well with the two solutions obtained from the two-level representation and the two additional solutions correspond to waves with no amplification.

In the mean the amplitudes of the waves with $m \geqq 5$ have relatively small values about 30° N, increase to a maximum value between 45 and 50° N and then decrease again to small values about 70° N. Furthermore the tilt of these waves seems to be negligible, at least in the belt from 40 to 60° N. Certainly the exact meridional variation of a wave with the wavenumber m must be described by a superposition of several Legendre functions P_n^m $(\sin \varphi)$, however for $5 \leqq m \leqq 7$ the above, crude variation is rather well described (in the belt 30—70° N) by the single function P_n^m $(\sin \varphi)$ with $n - m = 4$. In the following we consider especially the amplified solution of (17) with $n = 10$ as being representative for the wave with wavenumber 6.

Having neglected the meridional variation of the angular velocity of the zonal flow it seems reasonable to fix α as the mean value in the belt from 35 to 60° N. From the normal charts of November α then becomes at the 500-mb level: 16.4, at the 700-mb level: 10.1 and at the 1,000-mb level 2.5 degrees of longitude per day, leading to the values $\alpha_1 = 20$ and $\alpha_2 = 7.5$ degrees of longitude per day.

With these values of α and $q = \frac{110}{n(n+1)}$ (i.e. $\varkappa = 2.7 \cdot 10^{-12}$ m^{-2}) equation (18) becomes for $n = 10$

$$\gamma = (9.4 \pm 2.9i) \text{ degrees of longitude per day}$$

This value of the velocity of propagation agrees rather well with the value determined from Fig. 6 for the period 23 October to 5 November in which the mean angular velocity of the zonal flow corresponds nearly to the normal of November. Also the subsequent decrease in the velocity of propagation (18—30 November) is in accordance with the formula (18) (cf. Fig. 7).

For the amplified solution with $\gamma = 9.4 + 2.9i$ equations (17) yield

$$z_2' = (0.33 \div 0.45i) z_1'$$

Determining z' for the 500-mb level by linear interpolation we find that the amplitude of the wave in the thickness field from p_2 to p_1 becomes 0.96 times the amplitude at the 500-mb level. Further the wave in the thickness field is displaced 0.11 times the wavelength towards the west in relation to the wave at the 500-mb level. These conditions seem to be rather well in agreement with the mean conditions outlined above for the actual waves in the atmosphere.

REFERENCES

BOLIN, B., 1950: On the influence of the earth's orography on the general character of the westerlies. *Tellus* 2, pp. 184—195.

— 1953: Multiple-parameter models of the atmosphere for numerical forecasting purposes. *Tellus* 5, pp. 207—218.

CHARNEY, J. G., 1947: The dynamics of long waves in a baroclinic westerly current. *J. Meteor.* 4, pp. 135—162.

— and ELIASSEN, A., 1949: A numerical method for predicting the perturbations of the middle latitude westerlies. *Tellus* 1, 2, pp. 38—54.

— and PHILLIPS, N., 1953: Numerical integration of the quasi-geostrophic equations for barotropic and simple baroclinic flows. *J. Meteor.* 10, pp. 71—99.

EADY, E. T., 1949: Long waves and cyclone waves. *Tellus* 1, 3, pp. 33—52.

ELIASSEN, A., 1952: Simplified models of the atmosphere, designed for the purpose of numerical weather prediction. *Tellus* 4, pp. 145—156.

FJØRTOFT, R., 1950: Application of integral theorems in deriving criteria of stability for laminar flows and for the baroclinic circular vortex. *Geof. Publ.* 17, 6, 52 pp.

MINTZ, Y., 1951: The geostrophic poleward flux of angular momentum in the month of January 1949. *Tellus* 3, pp. 195—200.

SMAGORINSKY, J., 1953: The dynamical influence of large-scale heat sources and sinks on the quasi-stationary mean motions of the atmosphere. *Quart. J. R. Meteor. Soc.* 79, pp. 342—366.

STARR, V. P., and WHITE, R. M., 1952: Schemes fort he study of hemispheric exchange processes. *Quart. J. R. Meteor. Soc.* 78, pp. 407—410.

THOMPSON, P. D., 1953: On the theory of large-scale disturbances in a two-dimensional baroclinic equivalent of the atmosphere. *Quart. J. R. Meteor. Soc.* 79, pp. 51—69.

WHITE, R. M., and COOLEY, D. S., 1956: Kinetic-energy spectrum of meridional motion in the mid-troposphere. *J. Meteor.* 13, pp. 67—69.